ChemComm

Accepted Manuscript

ROYAL SOCIETY OF CHEMISTRY

rsc.li/chemcomm

View Article Online
DOI: 10.1039/C8CC00178B

Journal Name

COMMUNICATION

A target-induced logically reversible logic gate for intelligent and rapid detection of pathogenic bacterial genes

Received 00th January 20xx,
Accepted 00th January 20xx

DOI: 10.1039/x0xx00000x

www.rsc.org/

Jiankang Deng[a], Zhanhui Tao[a], Yaqing Liu[a*], Xiaodong Lin[a], Pengcheng Qian[a], Yanlong Lyu[a], Yunfei Li[a], Kejing Fu[a], and Shuo Wang[a,b*]

For the first time, a target (pathogenic bacterial gene)-induced logically reversible logic gate was constructed as intelligent biosensor, which has one-to-one mapping function and can rapidly distinguishall informationof the two targets, the presence of any target and the absence (or presence) of both of the targets,from the unique output signal pattern.

Construction of (bio)-molecular logic gates has attracted high attention from molecular computing and biosensing.[1-4] Noted that molecular logic gates report high "1" or low "0" output to implement data and information processing triggered by various input combinations, they are expected to be appropriate as intelligent molecular devices for disease diagnosis and even automatic therapy processing.[5-8] Meanwhile, the ability of logic gate making a "YES" or "NO" conclusion endows it charming application in situations where a rapid decision-making is critical, for example emergencies of food safety and viral infections, detection of chemical weapons on a battlefield, and rapid evaluation of multiple analytes.[9,10] Katz and co-workers constructed enzyme-based logic network architectures to assess injury situations.[8,11] In very recently, an AND gate was utilized to indicate the coexistence of the two inputs, and an OR gate was used to indicate the existence of each of the two inputs or both of them.[12] The investigations made great achievements for logic gate-based intelligent diagnosis. However, it is worthy of noting that the corresponding input vector cannot be wholly addressed only according to the output information of the build logic gates.

Among the Boolean logic systems, logically reversible logic gates, such as Feynman, Toffoli, Wilczek, and Fredkin gate, have one-to-one mapping function and can restore all the original input information from the unique output signal combination without any information loss or heat release.[12-15] That is quite different from chemically reversible logic gates which implement function to reset the logic operation accompanying on the basis of reversible chemical reaction with minimum heat liberation of kTxln2.[16,17] The merits of logically reversible gates endow them significant application not only in molecular computing but also in future nanomedicine and intelligent biosensors for making a rapid decision.[18-21] However, no logically reversible logic gate-based intelligent analysis has been experimentally validated, which inspired us to conduct investigation to improve the development of logic gate-based biosensing. Pathogenic bacteria seriously threaten public health and can cause significant economic loss.[22,23] The rapid and efficient detection of pathogenic bacterial genes is an important issue for food safety monitoring and public health supervision.[24] With a kind of gram-negative Enteropathogenic bacterium gene (*Lac Z*) and a kind of gram-positive Staphylococcal aureus bacterium gene (*mec A*) as the target inputs, herein, an enzyme-free and label-free logically reversible gate, Feynman gate, was constructed as intelligent biosensor to rapidly distinguish all the target information according to the unique output signal combination.

A Feynman gate can be realized by integrating an XOR and an IDENTITY in parallel, which requires two signal indicators. DNA-templated silver nanoclusters (DNA-AgNCs) with excellent photostability, biocompatibility, solubility and low cost have attracted increasing attention from extensive research fields.[25] The fluorescent properties of DNA-AgNCs are highly sensitive to their micro-environment, endowing DNA-AgNCs promising application in DNA computing and biosensing.[26,27] More strikingly, the direct use of DNA-AgNCs as a signal indicator presents advantages over organic dyes and quantum dots that not only can this direct use avoid the covalent label of signal indicator into DNA but also can make it convenient to be introduced into logic system via the DNA template.[27] To modulate the fluorescence of DNA-AgNCs, GO was introduced into the logic system and acted as a super nanoquencher to quench the fluorescence of the AgNCs via long-range resonance energy transfer. Interestingly, GO also

[a] Key laboratory of Food Nutrition and Safety (Ministry of Education), Tianjin Key Laboratory of Food Nutrition and Safety, Tianjin University of Science and Technology, Tianjin, 300457, China.E-mail: yaqingliu@tust.edu.cn
[b] Tianjin Key Laboratory of Food Science and Health, School of medicine, Nankai University, Tianjin, 300071, China.E-mail: wangshuo@nankai.edu.cn
†Electronic Supplementary Information (ESI) available: Materials and experimentaldetails. See DOI: 10.1039/x0xx00000x

View Article Online
DOI: 10.1039/C8CC00178B

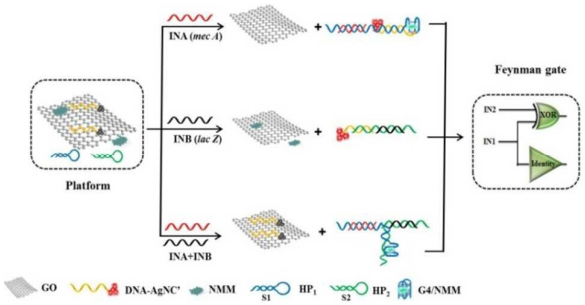

Scheme 1. The schematic principle of the Feynman gate-based intelligent detection of pathogen *mec A* and *Lac Z* genes.

has capability to distinguish single-stranded DNA from duplex or triplex DNA. Only single-stranded DNA is allowed to anchor to GO, which endows GO to be powerful material for modulating output signal.[28] Aside from DNA-AgNCs, NMM (N-methylmesoporphyrin IX) was selected as another signal indicator in that it presents remarkable structural selectivity for DNA with G-quadruplex (G4) configuration but not for triplexes, duplexes or single strand DNAs.[29] Once NMM is trapped on G4, its fluorescence is significantly augmented due to the formation of the G4/NMM complex.[30] By combining the signal modulation capability of G4 and advantages of DNA-AgNCs and GO, an enzyme-free and label-free Feynman gate was expected to be realized with simple operation.

Scheme 1 outlines the operation principle of the Feynman gate-based intelligent detection of pathogenic bacterial genes. Herein, *Lac Z* gene and *mecA* gene were defined as the two inputs, IN1 and IN2. The DNA-AgNCs anchored on GO acted as the initial platform, which reported high or low output signal to implement the function of XOR gate. To ensure that the DNA-AgNCs responses to both *Lac Z* gene and *mec A* gene, two DNA strands with hairpin configuration, HP_1 and HP_2, were introduced into the system to meet the requirements of Feynman gate-controlled gene detection. At the initial state, AgNCs and NMM reported low fluorescence. Via the toe-hold replacement strategy, the added IN1 of *mecA* gene would hybridize with HP_1 to form duplex of $IN1/HP_1$, which would further hybridize with the DNA-AgNCs to form complex of $IN1/HP_1$/DNA-AgNCs. The releasing of DNA-AgNCs from GO surface recovered fluorescence of the AgNCs. Similarly, the added IN2 of *Lac Z* gene would hybridize with HP_2 and DNA-AgNCs in sequence to form complex of $IN2/HP_2$/DNA-AgNCs, recovering fluorescence of the AgNCs. The difference was that $IN1/HP_1$/DNA-AgNCs could form G4 configuration while $IN2/HP_2$/DNA-AgNCs could not. In the coexistence of IN1 and IN2, the formed duplex of $IN1/HP_1$ and $IN2/HP_2$ would prefer to hybridize together to generate complex of $IN1/HP_1/HP_2$/IN2, companying the formation of G4 configuration due to the hybridization of HP_1 and HP_2. In this case, DNA-AgNCs was leaved on the GO surface. The fluorescence of NMM was significantly augmented by the formed G4. The outputs of AgNCs and NMM modulated by the inputs were related to the XOR and IDENTITY gate functions respectively. All the DNA sequence can be found from Table S1 in supporting information (SI).

The designed DNA interactions were validated by conducting native polyacrylamide gel electrophoresis (PAGE) experiments. As illustrated in Fig. 1A, the belts represented the individual DNA strands of IN1, IN2, DNA-AgNCs, HP_1 and HP_2 from Lane 1 to Lane 5, respectively. In the mixture of IN1 and HP_1, a new belt appeared at a different position, validating the formation of duplexes of $IN1/HP_1$ (Lane 6), which could further hybridize with DNA-AgNCs to form a complex of $IN1/HP_1$/DNA-AgNCs (Lane 8). The coexistence of IN2 and HP_2 resulted in the formation of the duplex of $IN2/HP_2$ (Lane 7), which could further hybridize with DNA-AgNCs to generate a complex of $IN2/HP_2$/DNA-AgNCs (Lane 9). In the coexistence of IN1, IN2, HP_1, HP_2 and DNA-AgNCs, they would hybridize together to form a complex of $IN1/HP_1/HP_2$/IN2, which was validated by the new belt in Lane 10. As control experiment, the HP_1, HP_2, and DNA-AgNCs did not hybridize with each other in the absence of *mec A* or *Lac Z* gene (See Fig. S1 in SI). Meanwhile, the *mec A* or *Lac Z* gene did not hybridized with DNA-AgNCs in the absence of HP_1 and HP_2, which was validated by the PAGE results (See Fig. S1 in SI).The formation of the G4 configuration was validated by conducting circular dichroism (CD) experiments, Fig. 1B. The CD spectra of IN1 (a), IN2 (b), DNA-AgNCs (c), HP_2 (d) and HP_1 (e) were found to have relative low amplitude, suggesting a random DNA structure.[31]In the coexistence of IN1, HP_1 and DNA-AgNCs, two obvious peaks were found at 246 nm and 265 nm from the CD spectrum (f). This feature was representative of the G4 with a parallel configuration.[31] In the coexistence of IN2, HP_2 and DNA-AgNCs, the CD spectrum was found to have a low amplitude (g), indicating that no G4 configuration was formed. When adding IN1 and IN2 into the mixture of HP_1, HP_2 and DNA-AgNCs, the G4 with a parallel configuration was generated, which was discerned from the positive peak at 265 nm and negative peak at 246 nm (h). The results validate that the G4 configuration was generated as expected.

The Feynman gate-based intelligent detection according to its one-to-one mapping function was explored by monitoring the fluorescence signals of DNA-AgNCs and NMM to respond the required XOR and IDENTITY gates in parallel. The DNA-AgNCs contained two regions, a cytosine-rich segment template AgNCs region acting as a signal indicator and a single-strand DNA region acting as input-recognizing region. When free of any input (0, 0), the fluorescence of DNA-AgNCs was

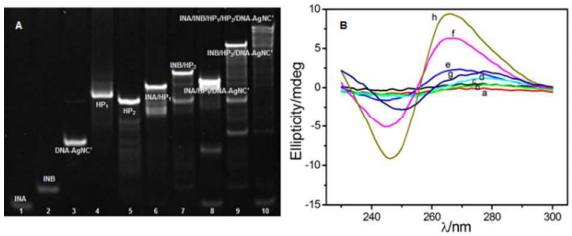

Fig. 1 (A) Polyacrylamide gel analysis of the DNA strands used in the Feynman logic gate-controlled detection. Lane 1: IN1; Lane 2: IN2; Lane 3: DNA-AgNCs; Lane 4: HP_1; Lane 5: HP_2; Lane 6: $IN1/HP_1$; Lane 7: $IN2/HP_2$; Lane 8: $IN1/HP_1$/DNA-AgNCs; Lane 9: $IN2/HP_2$/DNA-AgNCs; Lane 10: $IN1/HP_1/HP_2$/IN2+DNA-AgNCs. (B)The circular dichroism spectra of IN1 (a), IN2 (b), DNA-AgNCs (c), HP_2 (d), HP_1 (e), $IN1/HP_1$/DNA-AgNCs (f), $IN2/HP_2$/DNA-AgNCs (g), and $IN1/HP_1/HP_2$/IN2+DNA-AgNCs (h).

View Article Online
DOI: 10.1039/C8CC00178B

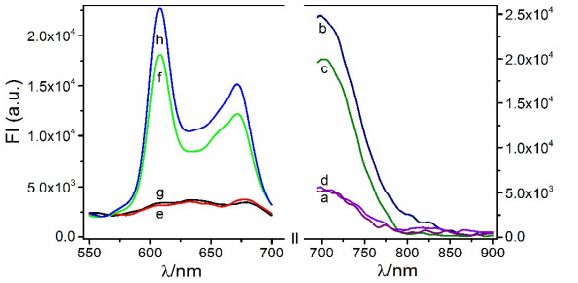

Fig. 2 The fluorescence responses of NMM and DNA-AgNCs in the absence of the two inputs (a, e), in the presence of *mec A* (b, f), in the presence of *Lac Z* (c, g), and in the presence of *mec A* and *Lac Z* (d, h).

quenched by GO, generating a dim fluorescence output signal (Fig. 2 (a)). The HP_1 contained a G-rich segment (GGGTGGGTGGG) at the 3'-terminal, which was embedded into the stem part to inhibit the formation of the G4 configuration. The HP_2 was designed not to form G4 configuration. Thus, a low fluorescent signal of NMM was monitored in the absence of any input (Fig. 2 (e)). The IN1, *mec A* gene, could hybridize with HP_1, transferring the hairpin structure to the duplex structure of IN1/HP_1 with a liberated segment of S1 and a G-rich segment of (GGGTGGGTGGG). S1 segment could hybridize with the input-recognition segment of the DNA-AgNCs. The DNA-AgNCs was then stripped from the GO, resulting in an obvious fluorescence signal, Fig. 2 (b). Meanwhile, the G-rich segment (GGGTGGGTGGG) at 3'-terminal of HP_1 formed a G4 configuration with the (GGG) segment of DNA-AgNCs. Complexes of G4/NMM were then generated to emit an outstanding fluorescence (Fig. 2 (f)). The IN2, *Lac Z* gene, could hybridize with HP_2, transferring the hairpin structure of HP_2 to duplex structure of IN2/HP_2 with a liberated segment of S2. The S2 segment was then hybridized with the input-recognition segment of the DNA-AgNCs to release AgNCs from the GO, restoring the fluorescence of AgNCs (Fig. 2 (c)). In this case, no G4 was formed through the hybridization. Thus, a low output signal of NMM was monitored (Fig. 2 (g)). In the coexistence of the two inputs, the formed IN1/HP_1 and IN2/HP_2 would hybridize together to form complexes of IN1/HP_1/HP_2/IN2 since the affinity of HP_1/HP_2 was higher than that of HP_1/DNA-AgNCs or HP_2/DNA-AgNCs. The DNA-AgNCs were still anchored on the GO surface, reporting a dim fluorescence (Fig. 2 (d)). Meanwhile, the hybridization of HP_1 and HP_2 generated the G4 construction to trap NMM, augmenting the fluorescence of NMM (Fig. 2 (h)). To establish optimal conditions, the concentrations of GO and DNA strands and the incubation time were experimentally optimized, which could be found from the supporting information (see Fig. S2-S5 in SI).

The overall fluorescence behaviours of the DNA-AgNCs-related XOR gate and the NMM-related IDENTITY gate within the framework of logic operation were summarized to clearly indicate the Feynman gate function. The fluorescent intensities of AgNCs at 699 nm and NMM at 609 nm were plotted as column bars against the input combinations and presented in Fig. 3A and 3B, respectively. Following the approach used in electronics, the output threshold values with an undefined

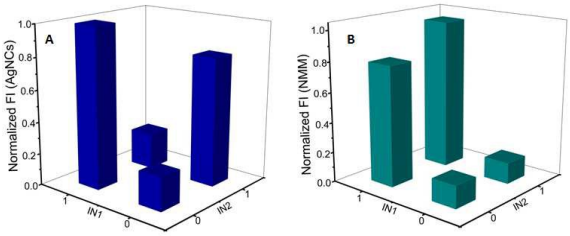

C

Inputs		Outputs	
IN1 (*mec A*)	IN2 (*Lac Z*)	NMM	AgNCs
0	0	0	0
1	0	1	1
0	1	0	1
1	1	1	0

Fig. 3 The fluorescent intensity of DNA-AgNCs at 699 nm (A) and NMM at 609 nm (B) against the input combinations. The corresponding truth table of the Feynman gate (C).

range were defined as "1" or "0" when the normalized fluorescence intensities of signal indicator at its maximum wavelength are higher than 0.3 or lower than 0.25, respectively. The presence or absence of input was defined as the input logic value of "1" or "0", respectively. A corresponding truth table (Fig. 3C) was produced, which met the feature of a Feynman logic gate.

Limit of detections of *mec A* and *Lac Z* in buffer solution (Fig. S6 in SI) and detection in biologically relevant sample (Fig. S7 in SI) have been evaluated. A reliable threshold value should be determined for logic gate-based analysis system.[32] Herein, the lowest concentrations in practical measurements (200 pM for *Lac Z* and 100 pM for *mec A*) were defined as input logic "1" while the absence of the target inputs was defined as logic "0". The corresponding fluorescent responses were defined as the thresholds for the output logic values to implement one-to-one mapping function of Feynman gate. To be easily understood, the pattern of Boolean output values of NMM against the Boolean output values of AgNCs was plotted as Fig. 4. If the Feynman gate reports Boolean output value of (0, 0), it indicates that neither *Lac Z* gene nor *mec A* gene exists in the sample. If Boolean output value of (1, 1) is read from the Feynman gate, one can conclude that the sample contains only

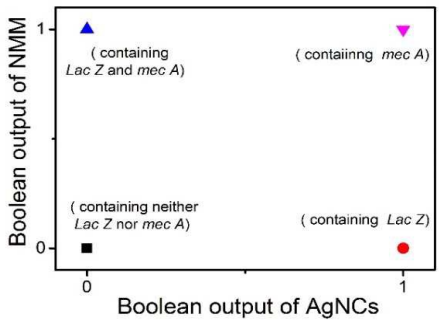

Fig. 4 The pattern of Boolean output value of NMM against the Boolean value of DNA-AgNCs in the absence of *mec A* and *Lac Z* genes (square), in the presence of *mec A* and *Lac Z* genes (up-triangle), *mec A* gene (down-triangle), *Lac Z* gene (dot).

View Article Online
DOI: 10.1039/C8CC00178B

mec A gene. If the logic sensing system reports a low Boolean output value of NMM and a high Boolean value of AgNCs, (0, 1), indicating only *Lac Z* gene exists in the sample. If Boolean out value of (1, 0) is monitored from the Feynman gate, suggesting both the *mec A* gene and *Lac Z* gene exist in the sample. Thus, the whole set combination of *mec A* gene and *Lac Z* gene, (0, 0), (0,1), (1, 0) and (1, 1), can be rapidly identified by direct reading the output pattern of the Feynman gate without any information loss or energy consumption. This identification presents advantages over the irreversible logic gate.[27] For example, a two-input AND gate only can identify the coexistence of the two inputs (1, 1) by reporting a high output logic value of "1". While it cannot further distinguish the other input combinations of (0, 0), (1, 0) and (0, 1) since the low output logic value of "0" is read in the three cases. For an OR gate-based analysis, each of the two inputs or both of them can result in high output signal. It can only distinguish the absence of both inputs (0, 0) with low output signal while cannot further distinguish whether its high output signal is caused by the state of (1, 0), (0, 1) or (1, 1).

In conclusion, the utilization of target-induced Feynman gate as intelligent biosensor has been experimentally validated for the first time with pathogenic bacterial genes (*mec A* gene and *Lac Z* gene) as the two inputs. The one-to-one mapping function of the Feynman gate endows it capability to distinguish all original input patterns of pathogenic genes from the corresponding outputs without any information losing. The Boolean output values , (0, 0), (0, 1), (1, 0), and (1, 1), are assigned to the cases of the absence of *mec A* and *Lac Z* genes, the presence of *mec A* and *Lac Z* genes, the presence of *Lac Z* genes, and the presence of *mec A*, respectively. The developed Feynman gate-based biosensing system presents significant potential applications in research fields where requires a rapid decision-making such as emergency diagnosis and food safety evaluation. The logic operation is entirely based on DNA hybridization and implemented in a label-free and enzyme-free condition, simplifying operation processing and eliminating waste accumulation in the system. Meanwhile, the XOR and IDENTITY gates required by the Feynman gate are triggered by the same two inputs. The investigation provides a cost-effective and straightforward way to construct advanced logic gates with high reproducibility and would be beneficial to the integration of multiple molecular devices to implement advanced computational processing.

This work is supported by the National Natural Science Foundation of China (No. 21775108 and No. 21575138). China International Science and Technology Cooperation Based of Food Nutrition/Safety and Medicinal Chemistry. The Tianjin Municipal Science and Technology Commission (Project No. 16PTSYJC00130). The International Science and Technology Cooperation Program of China (Project No. 2014DFR30350).

Conflicts of interest

There are no conflicts to declare.

Notes and references

1 R. M. Zadegan, M. D. E. Jepsen, L. L. Hildebrandt, V. Birkedal and J. Kjems, Small, 2015, **11**, 1811-1817.
2 Y. V. Gerasimova and D. M. Kolpashchikov, *Angew. Chem. Int. Ed.*, 2016, **55**, 10244-10247.
3 J. H. Chen, S. G. Zhou and J. L. Wen, *Angew. Chem. Int. Ed.*, 2015, **54**, 446-450.
4 H. L. Li, W. Hong, S. J. Dong, Y. Q. Liu and E. K. Wang, *Acs Nano*, 2014, **8**, 2796-2803.
5 E. Katz, J. Wang, M. Privman and J. Halamek, *Anal. Chem.*, 2012, **84**, 5463-5469.
6 J. Halamek, J. R. Windmiller, J. Zhou, M. C. Chuang, P. Santhosh, G. Strack, M. A. Arugula, S. Chinnapareddy, V. Bocharova, J. Wang and E. Katz, *Analyst*, 2010, **135**, 2249-2259.
7 Z. Xie, L. Wroblewska, L. Prochazka, R. Weiss and Y. Benenson, *Science*, 2011, **333**, 1307-1311.
8 K. M. Manian, J. Halámek, M. Pita, J. Zhou, T. K. Tam, P. Santhosh, M. C. Chuang, J. R. Windmiller, D. Abidin, E. Katz and J. Wang, *Biosens. Bioelectron.*, 2009, **24**, 3569-3574.
9 J. R. L. Ehrenkranz, *Epidemiol.*, 2002, **13**, S15-S18.
10 V. Kumar and M. P. Kaushik, *Analyst*, 2011, **136**, 5151-5156.
11 J. Halamek, V. Bocharova, S. Chinnapareddy, J. R. Windmiller, G. Strack, M. Chuang, J. Zhou, P. Santhosh, G. V. Ramirez, M. A. Arugula, J. Wang and E. Katz, Mol. *Biosyst.*, 2010, **6**, 2554-2560.
12 K. Morihiro, N. Ankenbruck, B. Lukasak and A. Deiters, *J. Am. Chem. Soc.*, 2017, **139**, 13909-13915.
13 J. Klein, T. Leete and H. Rubin, *Biosystems*, 1999, **52**, 15-23.
14 P. Remón and R. Ferreira, J. M. Montenegro, R. Suau, E. Pérez-Inestrosa and U. Pischel, *Chem. Phys. Chem.*, 2009, **10**, 2004-2007.
15 C. Y. Zhou, K. Wang, D. Q. Fan, C. T. Wu, D. L. Liu, Y. Q. Liu and E. K. Wang, *Chem. Commun.*, 2015, 51, 10284-10286.
16 R. Landauer, *IBM J. Res. Dev.*, 1961, **5**, 183-191.
17 A. J. Genot, J. Bath and A. J. Turberfield, *J. Am. Chem. Soc.*,2011, **133**, 20080-20083.
18 F. Moseley, J. Halámek, F. Kramer, A. Poghossian, M. J. Schöning and E. Katz, *Analyst*, 2014, **139**, 1839-1842.
19 R. Orbach, F. Remacle, R. D. Levine and I. Willner, *Proc. Natl. Acad. Sci. U. S. A.*, 2012, **109**, 21228-21233.
20 B. E. Fratto and E. Katz, *Chem. Phys. Chem.*, 2016, **17**, 1046-1053.
21 B. E. Fratto and E. Katz, *Chem. Phys. Chem.*, 2015, **16**, 1405-1415.
22 H. X. Yuan, Z. Liu, L. B. Liu, F. T. Lv, Y. L. Wang and S Wang, *Adv. Mater.*, 2014, **26**, 4333-4338.
23 C. H. Luo, H. Tang, W. Cheng, Li Yan, D. C. Zhang, H. X. Ju and S. J. Ding, *Biosens. Bioelectron.*, 2013, **48**, 132-137.
24 F. Q. Li, Z. G. Yu, H. C. Qu, G. L. Zahng, H. Yan, X. Liu and X. J. He, *Biosens. Bioelectron.*, 2015, **68**, 78-82.
25 E. G. Gwinn, P. O'Neill, A. J. Guerrero, D. Bouwmeester and D. K. Fygenson, *Adv. Mater.*, 2008, **20**, 279-283.
26 H. C. Yeh, J. Sharma, J. J. Han, J. S. Martinez and J. H. Werner, *Nano Lett.*, 2010, **10**, 3106-3110.
27 D. Q. Fan, J. B. Zhu, Y. Q. Liu, E. K. Wang and S. J. Dong, *Nanoscale*, 2016, **8**, 3834-3840.
28 K. Wang, J. T. Ren, D. Q. Fan, Y. Q. Liu and E. K, Wang, *Chem. Commun.*, 2014, **50**, 14390-14393.
29 S. S. Oh, K. Plakos, X. H. Lou, Y. Xiao and H. T Soh, *Proc. Natl. Acad. Sci. U. S. A.*, 2010, **107**, 14053-14058.
30 H. Li, J. Ren, Y. Liu and E. Wang, *Chem. Commun.*, 2014, **50**, 704-706.
31 P. Agarwala, S. Pandey and S. Maiti, Biochim. Biophys. Acta, 2014, **1840**, 3503–3510
32 M. Chuang, J. R. Windmiller, P. Santhosh, G. Valdes Ramırez, E. Katz and J. Wang, Chem. Commun., 2011, **47**, 3087–3089

View Article Online
DOI: 10.1039/C8CC00178B

Table of Contents Entry

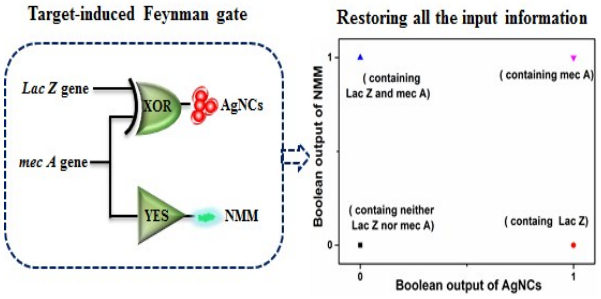

A target-induced Feynman gate acts as intelligent biosensor to distinguish all information of the targets from the output signal patterns.